An OFDM-MIMO Distributed Acoustic Sensing over Deployed Telecom Fibers

Christian Dorize[1], Sterenn Guerrier[1], Elie Awwad[2], Peter A. Nwakamma[1], Haik Mardoyan[1], Jérémie Renaudier[1]

[1] *Nokia Bell Labs Paris-Saclay, 1 route de Villejust, 91620 Nozay, France,*

[2] *Department of Communications and Electronics, TELECOM Paris, 19 Place Marguerite Perey, 91120 Palaiseau, France*

Christian.dorize@nokia-bell-labs.com

Abstract: We demonstrate the performance of a novel multi-carrier MIMO fiber sensing interrogator based on OFDM approach. Over an installed telecom fiber cable, coherent fading is mitigated by means of a purely digital subcarrier combiner.

1. Introduction

Distributed acoustic sensors have become a hot topic in many fields, from biomedical sensing to earthquake monitoring. In the specific context of smart cities, exploiting already-deployed telecom fibers as distributed sensors is an appealing alternative to deploying dedicated fibers to perform distributed acoustic sensing (DAS), which is in-turn more cost effective than installing a multitude of independent sensors [1,2]. The detection accuracy in recent works over deployed infrastructure may reach several meters, but with limited sensitivity. In case of applications where fine sensitivity and spatial resolution are jointly needed, coherent fading in phase optical domain reflectometry (ϕ-OTDR) is an issue since it degrades the sensor performance at random locations. To overcome it, a common solution is to use frequency diversity at the transmitter, as the random fading locations depend on the optical interrogation frequency [3]. Also, [4] recently showed that fading could be continuously mitigated by tracking the most reliable probe frequency in time.

Based on the recent polarization-independent coherent-MIMO sensing method [5], we introduce here a purely digital OFDM based multi-carrier interrogator that requires a simplified optical setup including a single highly coherent laser source. This technique allows to probe an optical fiber sensor with the benefits of frequency diversity and with a tunable number of subcarriers, without any modification to the optical setup. The sensing performance of such an interrogation method is tested over deployed fiber cables to detect dynamic events. It is demonstrated that the use of OFDM based multi-carrier together with coherent-MIMO interrogation mitigates the problem of Rayleigh fading points (or "coherent fading"). This is illustrated here by tracking a vehicle driving near a telecom cable.

2. Theory

Our fully digital spectral diversity approach relies on a P-subcarrier OFDM scheme. Each subcarrier is loaded with the same polarization diversity binary probing time codes, as for single carrier reference case [6]. The OFDM flow constructed after Inverse Fast Fourier Transform (IFFT) is made of a {-1,0,+1} alphabet and is transmitted over the fiber through a polarization diversity Mach Zehnder modulator (MZM) at a symbol rate f_{symb} equal to P times the subcarrier rate. At the coherent receiver side, FFT is performed per polarization axis onto each received OFDM symbol to separate the information per subcarrier. Each subcarrier information is then independently correlated with the polarization diversity time codes used at the transmitter side [6]. We finally get backscattered channel estimations under the form of Jones matrices $H_{t,d,sc}$ at each time, distance and sub-carrier index. Notice that for any given (t,d) pair, the Jones matrix responses from the P subcarriers are naturally synchronized thanks to the OFDM coding scheme with their intensity responses made of different Rayleigh backscatter contributions. It results in different Rayleigh fadings per subcarrier, which is exploited here to reduce this effect through a combination of the subcarrier responses. We now introduce a metric to quantify how much a fiber segment i is subject to coherent fading. Any backscattered matrix $\mathbf{H}$ at distance index i is defined as $\mathbf{H}_i = A_i\, p_i \mathbf{U}_i^t\, \mathbf{M}\mathbf{U}_i$ [5] where $\mathbf{U}_i$ is a unitary forward transmission matrix and $\mathbf{M}$ is the reflection matrix, assumed perfect here. A_i is the attenuation along the fiber, and p_i is the common phasor of the matrix derived from the backscatterer positions along the fiber. The product $\mathbf{U}_i^t\mathbf{M}\mathbf{U}_i$ is unitary [5], Rayleigh fading is thus enclosed in the sole modulus of $A_i\, p_i$, simply derived from the determinant modulus of H_i, leading to the reliability metric $R_i = |\det(\mathbf{H}_i)| = |A_i\, p_i|^2$. The lower R, the lower the global backscattered intensity over the two polarization axes and so the lower the reliability of the estimated phase $\phi_i = \arg(\det(\mathbf{H}_i))$. In this work, we use the R metric to compare Rayleigh fading from the single carrier MIMO reference case and the novel OFDM based multicarrier MIMO one. For this latter case, and at every (t,d) pair, the combination of subcarriers is based on a

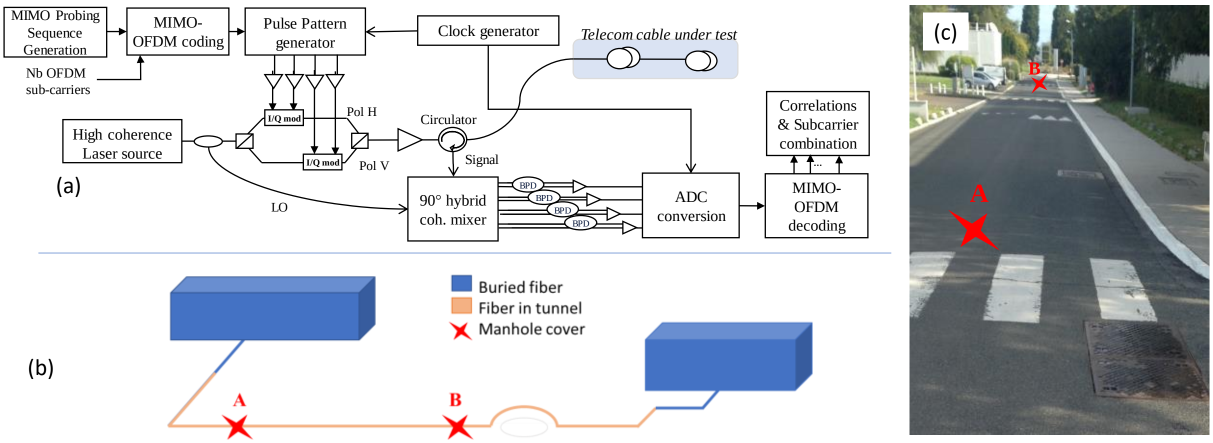

Figure 1: (a) Lab interrogator setup (b) Path of deployed fiber (c) Road under which the fiber is deployed

rotated-vector-sum summation [7] of the P subcarriers, which is allowed since the P subcarrier matrices encounter the same polarization state evolution. This in phase summation maximizes the SNR of the combined information.
For sake of fair comparison between the single-carrier and OFDM cases, we use a common electrical bandwidth B_e, determined by the symbol rate. With the multicarrier approach, the rate per subcarrier is P times lower than that of the transmitted OFDM flow, which degrades the initial spatial resolution $SR = c_f / 2. f_{symb}$, where c_f is the speed of light in the fibre, by a P factor compared with the single carrier case. Also, the subcarrier code length is adjusted to provide the same duration T_{code} as for the single carrier case, so preserving the mechanical bandwidth $B_m = 1/T_{code}$.

3. Experiment

A 700m-long coated cable enclosing six single mode fibers (SMF) is deployed between two buildings on an enterprise campus. It is buried approximately 0.6m under an asphalt road for most of the distance, first in a small pipe together with water and electricity lines and then fixed to the wall of a 2-m high underground tunnel, see Fig.1. Firstly, one cable fiber is interrogated at a symbol rate of 50MHz without any vehicle in motion on the road, successively through single-carrier, OFDM with 2 subcarriers and OFDM with 4 subcarriers interrogations.

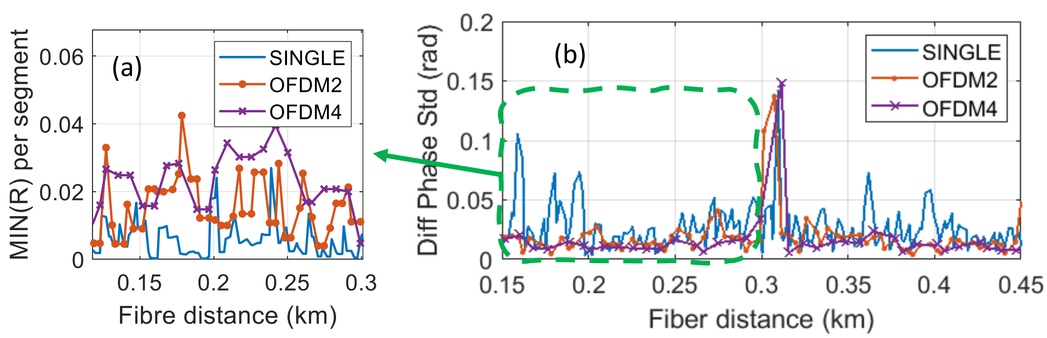

Figure 2: static measurements on the deployed fiber cable (a) Minimum R value (b) Standard deviation of phase

The reliability and sensitivity results are displayed in Figure 2 for the [150-450]m cable section. Fig.2a shows the minimum reliability value R in time for each fiber segment at the beginning of this cable section. This metric is chosen since phase estimation artefacts occur more likely as R gets close to 0, thus affecting the sensitivity, which is especially noticeable in absence of external perturbation. Here, the overall reliability clearly increases with the number of subcarriers. Fig.2b shows the system sensitivity through the standard deviation of the differential phases captured along the same cable section. Beyond the sensitivity, stationary disturbances such as machinery noise, water pipes, echoes in the tunnel locally induce backscattered phase variations. The peak at 310m observed on every measurement in Fig.2b comes from the noise of a water pipe crossing the fiber path. When P increases, the number and levels of false alarms shrink such that the OFDM4 case, thanks to its higher sensitivity, further highlights the mechanical event and more generally enhances the detection performances.

Fig.1a details the system setup whereas Fig.1b&c show the 700m long fiber cable path between the two buildings and a picture focus on the [150-450]m cable section where the dynamic experimentation takes place respectively. The optical part setup is our dual-polarization interrogation coherent (MIMO) phase OTDR with a highly stable laser source at 1536nm mounted in a homodyne configuration and already introduced in previous work [5,7]. The novelty here lies on the multi-carrier digital processing blocks. At the transmitter side, the polarization-division-multiplexed OFDM signals are calculated from the selected code length [6] and taking into account the desired number of subcarriers prior to injection into the MZM. At the receiver side, OFDM demodulation is performed through an FFT for both polarization channels. Correlation is then applied per subcarrier and followed by the combination of Jones matrices as previously detailed. With the OFDM spectral diversity approach, the overall numerical complexity of the receiver does not increase with the selected subcarrier number since a higher number of correlations to perform is compensated by the shorter vector lengths to correlate. The spatial resolution loss by a P factor is the only shortcoming here.

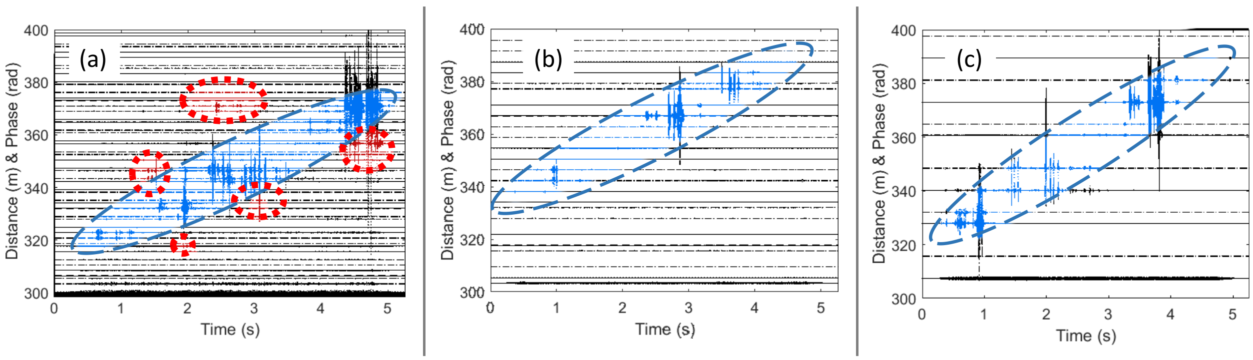

Figure 3: Evolution of phase in the time-distance plane, successive measurements for single-carrier (a) and OFDM2,4 (b,c) interrogations. Blue/dashed: on vehicle trajectory - Red/dotted: unreliable zones or false alarms.

Secondly, the fiber response is tested while a vehicle passes at a stable speed of 40km/h between A (t=0s, d=350m) and B (t=4s, d=390m) locations (see Fig.1c). Fig.3 displays the phase response in the time versus distance plane for the three tested configurations. The vehicle trajectory is highlighted by the blue spot whereas false alarms, concentrated in the single carrier case, appear in red. We checked that these local artefacts originated from coherent fading by noticing that they all correspond to local minima of the reliability metric. With OFDM measurements, the false alarms vanish while the vehicle trajectory is getting more visible with the increase of the number of subcarriers. Therefore, this latter parameter fixes the trade-off between the targeted coherent fading reduction and spatial resolution (in our case, 2, 4 and 8m resp.), and must be adjusted according to the application case requirements.

4. Conclusion

We introduced a purely digital frequency diversity scheme to tackle the speckle noise encountered in coherent phase OTDR. This MIMO-OFDM innovative approach to fiber sensing was shown to strongly reduce the false alarms induced by coherent fading, thus further enhancing the detection performance of mechanical events. It was experimentally highlighted by tracking a vehicle moving in the surrounding of a standard telecom fiber cable.

5. References

[1] G. A. Wellbrock et al., 'First Field Trial of Sensing Vehicle Speed, Density, and Road Conditions by using Fiber Carrying High Speed Data', in 2019 Optical Fiber Communications Conference and Exhibition (OFC), Mar. 2019, pp. 1–3

[2] T. J. Xia et al., 'First Proof That Geographic Location on Deployed Fiber Cable Can Be Determined by Using OTDR Distance Based on Distributed Fiber Optical Sensing Technology', in Optical Fiber Communication Conference (OFC) 2020, San Diego, California, 2020, p. Th3A.5, doi: 10.1364/OFC.2020.Th3A.5.

[3] A. H. Hartog et al., 'The use of multi-frequency acquisition to significantly improve the quality of fibre-optic-distributed vibration sensing', Geophysical Prospecting, vol. 66, no. S1, pp. 192–202, 2018, doi: 10.1111/1365-2478.12612.

[4] M. Zabihi et al., 'Continuous Fading Suppression Method for Φ-OTDR Systems Using Optimum Tracking Over Multiple Probe Frequencies', J. Lightwave Technol., vol. 37, no. 14, pp. 3602–3610, Jul. 2019, doi: 10.1109/JLT.2019.2918353.

[5] S. Guerrier, C. Dorize, E. Awwad, and J. Renaudier, 'Introducing coherent MIMO sensing, a fading-resilient, polarization-independent approach to ϕ-OTDR', Opt. Express, vol. 28, no. 14, p. 21081, Jul. 2020, doi: 10.1364/OE.396460.

[6] C. Dorize and E. Awwad, 'Enhancing the performance of coherent OTDR systems with polarization diversity complementary codes', Opt. Express, vol. 26, no. 10, p. 12878, May 2018, doi: 10.1364/OE.26.012878.

[7] D. Chen, Q. Liu, and Z. He, 'Phase-detection distributed fiber-optic vibration sensor without fading-noise based on time-gated digital OFDR', Opt. Express, vol. 25, no. 7, p. 8315, Apr. 2017, doi: 10.1364/OE.25.008315.